The Journal of Eukaryotic Microbiology
Published by the International Society of Protistologists

Journal of Eukaryotic Microbiology ISSN 1066-5234

ORIGINAL ARTICLE

Molecular Phylogeny of Marine Gregarine Parasites (Apicomplexa) from Tube-forming Polychaetes (Sabellariidae, Cirratulidae, and Serpulidae), Including Descriptions of Two New Species of *Selenidium*

Kevin C. Wakeman & Brian S. Leander

Departments of Botany and Zoology, Canadian Institute for Advanced Research, Program in Integrated Microbial Biodiversity, University of British Columbia, #3529 – 6270 University Blvd., Vancouver, British Columbia, V6T 1Z4, Canada

Keywords
Archigregarines; molecular systematics; single-cell PCR; trophozoites.

Correspondence
K.C. Wakeman, Departments of Botany and Zoology, Canadian Institute for Advanced Research, Program in Integrated Microbial Biodiversity, University of British Columbia, #3529 – 6270, University Blvd., Vancouver, British Columbia V6T 1Z4, Canada
Telephone number: +1 604 822 2474;
FAX number: +1 604 822 6089;
e-mail: wakeman.kevin@gmail.com

Received: 16 November 2012; revised 15 April 2013; accepted April 15, 2013.

doi:10.1111/jeu.12059

ABSTRACT

Selenidium is a genus of gregarine parasites that infect the intestines of marine invertebrates and have morphological, ecological, and motility traits inferred to reflect the early evolutionary history of apicomplexans. Because the overall diversity and phylogenetic position(s) of these species remain poorly understood, we performed a species discovery survey of *Selenidium* from tube-forming polychaetes. This survey uncovered five different morphotypes of trophozoites (feeding stages) living within the intestines of three different polychaete hosts. We acquired small subunit (SSU) rDNA sequences from single-cell (trophozoite) isolates, representing all five morphotypes that were also imaged with light and scanning electron microscopy. The combination of molecular, ecological, and morphological data provided evidence for four novel species of *Selenidium*, two of which were established in this study: *Selenidium neosabellariae* n. sp. and *Selenidium sensimae* n. sp. The trophozoites of these species differed from one another in the overall shape of the cell, the specific shape of the posterior end, the number and form of longitudinal striations, the presence/absence of transverse striations, and the position and shape of the nucleus. A fifth morphotype of *Selenidium*, isolated from the tube worm *Dodecaceria concharum*, was inferred to have been previously described as *Selenidium* cf. *echinatum*, based on general trophozoite morphology and host association. Phylogenetic analyses of the SSU rDNA sequences resulted in a robust clade of *Selenidium* species collected from tube-forming polychaetes, consisting of the two new species, the two additional morphotypes, *S.* cf. *echinatum*, and four previously described species (*Selenidium serpulae*, *Selenidium boccardiellae*, *Selenidium idanthyrsae*, and *Selenidium* cf. *mesnili*). Genetic distances between the SSU rDNA sequences in this clade distinguished closely related and potential cryptic species of *Selenidium* that were otherwise very similar in trophozoite morphology.

GREGARINE parasites within the genus *Selenidium* have retained several morphological and ecological traits inferred to be ancestral for apicomplexans as a whole, such as monoxenous lifecycles involving extracellular trophozoites (feeding stages) that feed by myzocytosis within the intestinal lumen of marine invertebrate hosts (Leander 2007, 2008; Schrével 1968, 1970, 1971a,b; Simdyanov and Kuvardina 2007). However, molecular phylogenetic data from this genus are rare, which severely limits our understanding of these evolutionarily significant parasites. Small subunit (SSU) rDNA sequences, for instance, are currently available from only seven of the approximately 60 described species of *Selenidium*, and it is expected that the vast majority of *Selenidium* species have yet to be discovered and characterized. As such, the phylogenetic relationships between *Selenidium* species

and other lineages of marine gregarines remain unclear (Leander 2007, 2008; Leander et al. 2003; Rueckert and Leander 2009; Wakeman and Leander 2012).

Selenidium species have been reported predominately from polychaete worms (e.g., spionids, sabellids, and serpulids) but have also been described from sipunculids, sea cucumbers, hemichordates, and tunicates (Levine 1971; Ray 1930; Rueckert and Leander 2009; Schrével 1971a; Wakeman and Leander 2012). The intestinal trophozoites are either spindle-shaped or vermiform and exhibit a type of bending motility that is reminiscent of nematodes. The cell shape, pattern of motility, and specific ultrastructural features associated with the trophozoite stage in *Selenidium* (e.g., an apical complex associated with myzocytosis and a robust corset of microtubules beneath the inner membrane complex) are most similar to the traits of apicomplexan sporozoites in general and, taken together, are indicative of the traditional "archigregarine" concept (Grassé 1953; Leander 2008; Mellor and Stebbings 1980; Schrével 1970, 1971a,b; Simdyanov and Kuvardina 2007; Stebbings et al. 1974; Vivier and Schrével 1964; Wakeman and Leander 2012). This concept promotes the inference that *Selenidium* species have retained several morphological, ecological, and life history traits from distant ancestors that provide compelling insights into the earliest stages of apicomplexan evolution (Barta and Thompson 2006; Cox 1994; Dyson et al. 1994; Leander 2007, 2008; Leander and Keeling 2003). Therefore, continued exploration of *Selenidium* diversity is expected to shed considerable light onto the deepest relationships within the phylogeny of apicomplexans and onto patterns of co-evolution between gregarine apicomplexans and marine metazoan hosts (Leander 2008; Rueckert and Leander 2009; Théodoridès 1984).

Unlike many species of terrestrial gregarines (from insect hosts), marine gregarines are particularly challenging to work with because they are generally encountered only as trophozoites and in low numbers within a small percentage of individual hosts that are difficult to obtain from oceanic environments (Wakeman and Leander 2013).

In this study, we discovered five different morphotypes of *Selenidium* isolated from the intestines of three different species of tube-forming polychaetes collected from the Pacific Ocean. These *Selenidium* isolates were compared with one another and with previously described species using a combination of molecular, ecological, and morphological data. SSU rDNA sequences were generated from single-cell (trophozoite) isolates that were first imaged with light microscopy. These data enabled us to evaluate cryptic diversity among gregarines, establish two new species of *Selenidium*, and link SSU rDNA sequences to a previously described species of *Selenidium*. These data underscored the practical advantages of DNA sequences in advancing the field of gregarine systematics and the importance of reciprocal reinforcement between molecular, morphological, and ecological data in building arguments for the establishment of new species (Leander 2008; Rueckert et al. 2011a,b; Wakeman and Leander 2013).

MATERIALS AND METHODS

Collection of host animals

Neosabellaria cementarium Moore, 1906 and *D. concharum* Örsted, 1843 were collected in February 2012 off rocks in Victoria, British Columbia, Canada while SCUBA diving at a depth of 10–20 m near Ogden Point 48°24′46.10″N 123°23′24.67″W and Clover Point 48°24′14.18″N 123°21′00.91″W, respectively. *Spirobranchus giganteus* Pallas, 1766 was purchased in March 2012 from J&L Aquatics, Burnaby, British Columbia, Canada. Host guts from seven, nine and four individuals of *N. cementarium*, *D. concharum* and *S. giganteus*, respectively, were removed with forceps and teased apart in seawater on a well slide. All gut material from *N. cementarium* and *D. concharum* was infected with gregarine parasites; 75% of the material (i.e., three individuals) from *S. giganteus* was infected.

Light microscopy

Hand-drawn glass pipettes were used to isolate and clean individual trophozoites using an inverted microscope (Zeiss Axiovert 200, Carl-Zeiss, Göttingen, Germany) attached to a PixeLink Megapixel color digital camera (PL-A662-KIT, Ottawa, Canada). Some isolates were photographed on well slides, washed in autoclaved, filtered seawater and collected for DNA extraction and single-cell PCR amplification (SC-PCR). Isolates were also photographed using a Leica DC 500 color camera attached to a Zeiss Axioplan 2 microscope (Carl-Zeiss, Göttingen, Germany); as noted below, some of these cells were also recovered for SC-PCR.

Scanning electron microscopy

Individual trophozoites were pooled in 2% glutaraldehyde on ice. A 10-μl polycarbonate membrane filter was placed within a Swinnex filter holder (Millipore Corp., Billerica, MA). Trophozoites were filtered onto the membrane using a syringe with distilled water, and the holder was placed in a small beaker (4 cm diam. and 5 cm tall) that was filled with distilled water. Ten drops of 1% OsO_4 were added to the opening of the filter holder, and the samples were postfixed on ice for 30 min. The syringe was used to slowly run distilled water over all samples. A graded series of ethanol washes (30%, 50%, 75%, 85%, 95%, and 100%) were then used to dehydrate the fixed cells using the syringe system. Following dehydration, the polycarbonate membrane filters containing the trophozoites were transferred from the Swinnex filter holders into an aluminum basket submerged in 100% ethanol in preparation for critical point drying with CO_2. The dried polycarbonate membrane filters containing the trophozoites were mounted on aluminum stubs, sputter coated with 5 nm gold and viewed under a Hitachi S4700 scanning electron microscope (Nissei Sangyo America, Ltd., Pleasanton, CA). Some SEM data were presented on a black background using Adobe Photoshop 6.0 (Adobe Systems, San Jose, CA).

DNA extraction, single-cell PCR amplification, and sequencing

Each of the single-cell isolates (13 total) were placed in a 1.5 ml eppendorf tube containing cell lysis buffer. Genomic DNA was extracted with the standard protocol provided by the MasterPure complete DNA & RNA purification kit (Epicentre Biotechnologies, Madison, WI). However, the final elution step was lowered to 4 μl, with the goal of concentrating extracted DNA prior to SC-PCR amplification. Outside primers, PF1 5′-GCGCTACCTGGTT GATCCTGCC-3′ and SSUR4 5′-GATCCTTCTGCAGGTT CACCTAC-3′ (Leander et al. 2003), were used in a 25 μl PCR with EconoTaq 2X Master Mix (Lucigen Corp., Middleton, WI). The following program was used on the thermocycler for the initial amplification: initial denaturation at 94 °C for 2 min, 35 cycles of denaturation at 94 °C for 30 s, annealing at 52 °C for 30 s, extension at 72 °C for 1 min 50 s, final extension 72 °C 9 min. Subsequently, internal primers F2 5′-GGTAGYGACAAGAAATAACAAC-3′ and R2 5′-GAYTACGACGGTATCTGATCGTC-3′ were paired with outside primers in a nested PCR using the following program on a thermocycler: initial denaturation for 94 °C for 2 min, 25 cycles of denaturation at 94 °C for 30 s, annealing at 55 °C for 30 s, extension at 72 °C for 1 min 30 s, final extension at 72 °C for 9 min. All SC-PCR products were separated on agarose gels and isolated using the UltraClean15 DNA Purification Kit (MO BIO, Laboratories, Inc., Carlsbad, CA), and cloned into a pCR 2.1 vector using a StrataClone PCR cloning kit (Aligent Technologies, Santa Clara, CA). Clones were screened for size and sequenced using vector primers and ABI Big-dye reaction mix. Novel sequences (i.e., one from each of the single-cell isolates) were identified using the National Center for Biotechnology Information's (NCBI) BLAST tool, confirmed with molecular phylogenetic analyses, and deposited in GenBank (KC110863–KC110875).

Molecular phylogenetic analyses

Two separate datasets were constructed de novo and analyzed in this study: (1) a comprehensive 82-taxon alignment (1,085 unambiguously aligned sites) containing a representative SSU rDNA sequence from each of the five *Selenidium* morphotypes described here, three dinoflagellate sequences (outgroup), and 74 sequences representing gregarine and other apicomplexan subclades and (2) a 17-taxon alignment (1,610 unambiguously aligned sites) containing the 13 *Selenidium* sequences generated in this study by SC-PCR (from five different morphotypes) and four sequences published previously from closely related *Selenidium* species. Both alignments were initially constructed using MUSCLE (Edgar 2004) and were subsequently edited using MacClade 4 (Maddison and Maddison 2000); gaps and ambiguously aligned regions were excluded from the analyses.

Jmodeltest 0.1.1 selected a GTR + I + Γ model of evolution under Akaike Information Criterion (AIC) and AIC with correction for both alignments (82-taxon alignment: proportion of invariable sites = 0.1820, gamma shape = 0.6230; 17-taxon alignment: proportion of invariable sites = 0.3290, gamma shape = 0.3770) (Posada and Crandall 1998). Garli0.951-GUI (www.bio.utexas.edu/faculty/antisense/garli/Garli.html) was used to infer a maximum likelihood (ML) tree and for ML bootstrap analyses (500 pseudoreplicates, one heuristic search per pseudoreplicate) (Zwickl 2006).

Bayesian posterior probabilities were calculated for both alignments using the following parameter on the program MrBayes 3.1.2. (Huelsenbeck and Ronquist 2001; Ronquist and Huelsenbeck 2003): (GTR [Lset nst = 6]; gamma distribution [of rate among sites] and Monte Carlo Markov Chains [starting trees = 4; default temperature = 0.2; generations = 7,000,000; sample frequency = 100; prior burn-in = 500,000 trees]; stop rule of 0.01 [i.e. when the average split deviation fell below 0.01, the program would terminate]). Burn-in was confirmed manually, and majority-rule consensus trees were constructed; posterior probabilities correspond to the frequency at which a given node is found in the post-burn-in trees. PAUP 4.0 (Swofford 1999) was used to calculate percent differences between the SSU rDNA sequences in the 17-taxon alignment. All alignments are available upon request.

RESULTS

Selenidium cf. *echinatum*

The trophozoites isolated from the gut material of *D. concharum* were spindle-shaped, 173 μm (95–205 μm; $n = 14$) long and 10 μm (8–11 μm; $n = 14$) wide (Table 1 and Fig. 1–4). The cells were capable of bending and twisting. The spherical nucleus had an average width of 10 μm ($n = 14$) and was positioned in the anterior-half of the trophozoites. Syzygy of gamonts was tail-to-tail (Fig. 5). The mucron terminated as a nipple-like projection at the anterior tip of the cell, where a single apical opening was observed (Fig. 6, 7). Five to six longitudinal striations were observed on one side of the cell (Fig. 7). Parasites on gold sputter-coated SEM stubs have been deposited in the Beaty Biodiversity Museum (Marine Invertebrate Collection) at the University of British Columbia, Vancouver, Canada. Museum Code – MI-PR124.

Selenidium neosabellariae n. sp.

Trophozoites isolated from the intestines of *N. cementarium* were elongate and vermiform in shape, 292 μm (125–350 μm; $n = 27$) long, and 11 μm (9–12 μm; $n = 27$) wide (Table 1 and Fig. 8–12). The spherical nucleus (10 μm; $n = 20$) was positioned in the center of the trophozoite cell (Fig. 8–11). The posterior end tapered to a fine point, and the base of a cone-shaped mucron was defined by a cluster of transverse striations (Fig. 12, 13). Five to six longitudinal striations were observed on one side of the cell (Fig. 12–14). Parasites on gold sputter-coated SEM stubs have been deposited in the Beaty Biodiversity Museum (Marine Invertebrate Collection) at

Table 1. Morphological comparisons of trophozoites between species within the *Selenidium* clade and the type species, *S. pendula*. *Species of Selenidium [italics font] are highlighted in bold.*

	Selenidium pendula (type)	*Selenidium idanthyrsae*	*Selenidium serpulae*	*Selenidium* cf. *mesnili*	*Selenidium boccardiellae*	***Selenidium* cf. *echinatum***	***Selenidium neosabellariae n. sp***	***Selenidium* sp. 1**	***Selenidium* sp. 2**	***Selenidium sensimae n. sp.***
Host	*Nerine cirratulus*	*Idanthyrsus saxicavus*	*Serpula vermicularis* (*contortuplicata*)	*Myxicola infundibulum*	*Boccardiella ligerica*	***Dodecaceria concharum***	***Neosabellaria cementarium***	***Spirobranchus giganteus***	***S. giganteus***	***S. giganteus***
Host tissue	Intestines	Intestines	Intestines	Intestines	Intestines	**Intestines**	**Intestines**	**Intestines**	**Intestines**	**Intestines**
Locality	E. Atlantic	W. Pacific	W. Pacific	W. Pacific	W. Pacific	**W. Pacific**	**W. Pacific**	**E. Pacific**	**E. Pacific**	**E. Pacific**
Trophozoite shape	Vermiform	Spindle-shaped, partially flattened	Spindle-shaped	Spindle-shaped	Spindle-shaped, partially flattened	**Spindle-shaped**	**Vermiform**	**Cylindrical**	**Spindle-shaped**	**Spindle-shaped**
Tophozoite size (L × W, μm)	180 × 30–40	450–543 × 9–11	100–150 × 7–25	85–157 × 18–24	87–250 × 10–12	**95–205 × 8–11**	**125–350 × 9–12**	**105–220 × 9–14**	**150–185 × 10–15**	**130–170 × 10–13**
Nucleus shape	Spherical	Spherical	Ellipsoidal	Ellipsoidal	Ellipsoidal	**Spherical**	**Spherical**	**Spherical**	**Ellipsoidal**	**Ellipsoidal**
Nucleus size (L × W, μm)	18–33 × 13–32	13–16 × 9–10	7–10 × 5–11	7–9 × 10–11	10–12 × 4–6	**10**	**10**	**10 × 4–6**	**10 × 4–6**	**10 × 4–6**
Position of nucleus	Middle	Middle to posterior-half	Anterior-half	Anterior to posterior	Anterior-half	**Anterior-half**	**Middle**	**Anterior**	**Middle**	**Middle**
Shape of posterior end	Pointed	Flat/pointed	Rounded	Rounded	Pointed	**Pointed**	**Pointed**	**Rounded**	**Spade-like**	**Blunt with indentation**
Number of longitudinal epicytic folds	20–30	20–22	14–23	22–24	10–12	**10–12**	**10–12**	**16–18**	**18–20**	**16–18**
Transverse surface folds	Unknown	Yes	Yes	Yes	No	**No**	**Yes**	**Unknown**	**Unknown**	**No**
Shape of mucron	Pointed	Pointed	Pointed to round	Pointed to round	Pointed	**Nipple-shaped**	**Nipple-shaped**	**Rounded to pointed**	**Nipple-shaped**	**Rounded to blunt**
Literature	Levine 1971; Schrével 1970	Wakeman and Leander 2012	Levine 1971; Leander 2006	Brasil 1909; Wakeman and Leander 2012	Wakeman and Leander 2012	**Caullery and Mesnil 1899; this study**	**This study**	**This study**	**This study**	**This study**

The bold indicates species presented in this study.

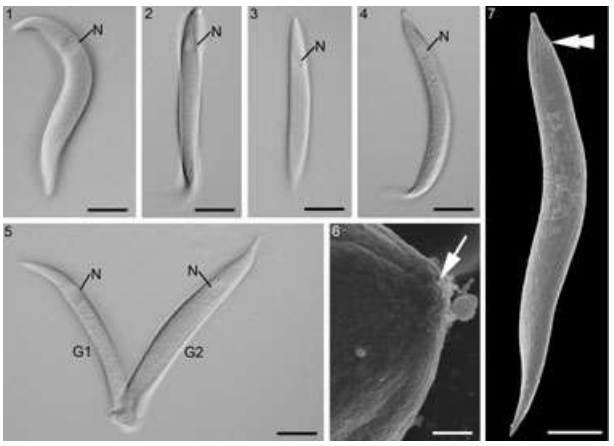

Figure 1–7 Differential interference contrast light micrographs (LM) and scanning electron micrographs (SEM) of the trophozoite stage of *Selenidium* cf. *echinatum* isolated from the intestines of *Dodecaceria concharum*. **1–4**. LMs showing the general spindle-shaped morphology of the trophozoites that were used for single-cell (SC) PCR. The nipple-like mucron is oriented upwards. The spherical nucleus (N) is positioned in the anterior region of the trophozoites. Longitudinal epicytic folds (arrowhead) run nearly the entire length of the trophozoite. **5.** LM showing two gamonts in tail-to-tail syzygy. **6.** High-magnification SEM showing the mucron region of the trophozoite with a single apical opening at the tip (arrow). **7.** SEM showing the general morphology of the trophozoite. Five to six relatively weakly developed epicytic folds (double arrowhead) run along the longitudinal axis on each side of the cell. Scale bars: 1–5 = 25 μm; 6 = 1 μm; 7 = 10 μm.

the University of British Columbia, Vancouver, Canada. Museum Code – MI-PR122.

Selenidium sensimae n. sp.

This species represented one of three trophozoite morphotypes isolated from the intestines of *S. giganteus*. These trophozoites were spindle shaped, 155 μm (130–170 μm $n = 11$) long, and 12 μm (10–13 μm; $n = 11$) wide (Table 1 and Fig. 15–18). An ellipsoidal nucleus (10 × 4–6 μm; $n = 11$) was centrally located in the cell. The posterior end of the cell tapered distinctly to a blunt point with a terminal indentation (Fig. 15–18); the anterior region of the cell either tapered to a blunt point or was rounded. There were eight to nine longitudinal striations observed on one side of the cell (Fig. 18). A row of micropores were positioned in the grooves between the epicytic folds and extended nearly the entire length of the cell (Fig. 19). Parasites on gold sputter-coated SEM stubs have been deposited in the Beaty Biodiversity Museum (Marine Invertebrate Collection) at the University of British Columbia, Vancouver, Canada. Museum Code – MI-PR123.

Selenidium sp. 1

This species represented one of three trophozoite morphotypes isolated from the intestines of *S. giganteus*. These trophozoites were relatively cylindrical in shape, elongate, measured 170 μm (105–220 μm; $n = 9$) long, and 13 μm

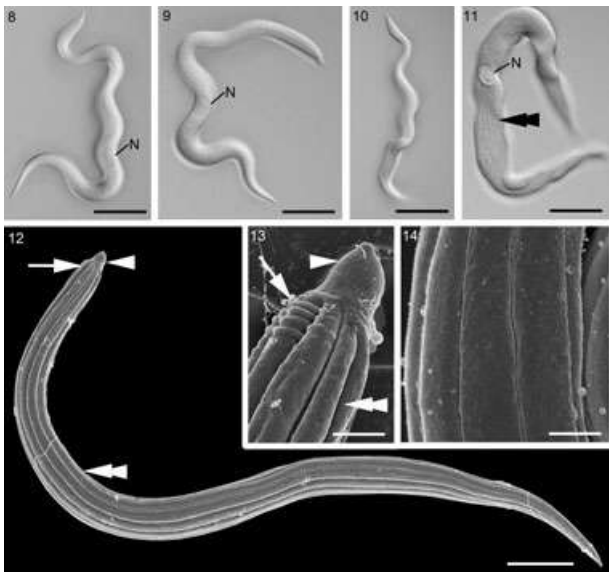

Figure 8–14 Differential interference contrast light micrographs (LM) and scanning electron micrographs (SEM) of the trophozoite stage of *Selenidium neosabellariae* n. sp. isolated from the intestines of *Neosabellaria cementarium*. **8–11.** LMs showing the vermiform and highly undulated morphology of the trophozoites with a nucleus (N) located in the center of the cell. Images 9–11 show the specific cells that were recovered for single-cell (SC) PCR. **12.** SEM showing the general vermiform-shape of the cell and epicytic folds (double arrowhead) that run along the longitudinal axis of the cell. The nipple-like mucron (arrowhead) is defined by a basal cluster of transverse striations (arrow). **13.** High-magnification SEM showing the mucron region (arrowhead) of the cell, the transverse striations (arrow), and the longitudinally arranged epicytic folds (double arrowhead). **14.** High magnification SEM of the longitudinally arranged epicytic folds. Scale bars: 8–11 = 35 μm; 12 = 10 μm; 13 = 3 μm; 14 = 1.5 μm.

(9–14 μm; $n = 9$) wide (Table 1 and Fig. 20–22), and displayed a dynamic ungulating movement.. The posterior and anterior ends of the cell were distinctly bulbous in shape. The spherical nucleus (10 μm; $n = 10$) was positioned in the anterior half of the cell (Fig. 20–22).

Selenidium sp. 2

This species represented one of three trophozoite morphotypes isolated from the intestines of *S. giganteus*. These trophozoites were spindle shaped, 160 μm (150–185 μm; $n = 13$) long, and 13 μm (10–15 μm; $n = 13$) wide (Table 1 and Fig. 23–25). The posterior end of the cell was distinctly spade-like in appearance (Fig. 23–25); the anterior region of the cell was pointed in association with a cone-shaped mucron. The ellipsoidal nucleus (10 × 4–6 μm; $n = 13$) was centrally located in the trophozoite cell. Nine to ten longitudinal striations were observed on one side of the cell (Fig. 23, 24).

Molecular phylogenetic analyses

Analyses of the 82-taxon alignment resulted in four relatively speciose clades of marine gregarines: crustacean

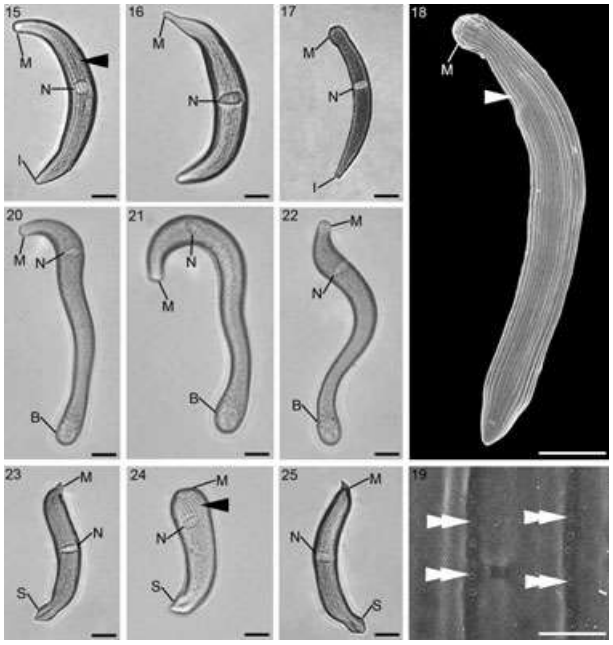

Figure 15–25 Differential interference contrast light micrographs (LM) and scanning electron micrographs (SEM) of the trophozoite stages of *Selenidium sensimae* n. sp., *Selenidium* sp. 1 and *Selenidium* sp. 2 isolated from the intestines of *Spirobranchus giganteus*. **15, 16.** LMs showing trophozoites of *S. sensimae* n. sp. that were used for single-cell (SC) PCR. The rounded mucron (M) is oriented upwards, the posterior end is blunt with a terminal indentation (I), and epicytic folds (arrowhead) run along the longitudinal axis of the cell. **17.** LM of a single-cell of *S. sensimae* n. sp. that was subsequently isolated and prepared for SEM. **18.** SEM showing the general cell morphology of *S. sensimae* n. sp. with eight to nine epicytic folds (arrowhead) that run along the longitudinal axis on one side of the cell. **19.** High-magnification SEM showing rows of pores (double arrowhead) running along the longitudinal axis of *S. sensimae* n. sp. **20–22.** LMs showing the general vermiform and cylindrical shape of *Selenidium* sp. 1 trophozoites that were isolated for SC-PCR. The nucleus (N) is positioned near the rounded mucron (M). The posterior end is distinctively bulbous (B) in shape. **23–25.** LMs showing the trophozoites of *Selenidium* sp. 2 that were isolated for SC-PCR. The pointed mucron (M) is oriented upwards and 18–20 epicytic folds (arrowhead) run along the longitudinal axis of the cell. An ellipsoidal nucleus (N) is positioned in the middle of the cell. The posterior end of the trophozoite is distinctly flattened and spade-shaped (S). Scale bars: 15–18, 19 = 1 μm, 20–25 = 10 μm.

gregarines, capitellid gregarines, lecudinids, and *Selenidium* species isolated from Pacific tube-forming polychaetes (Fig. 26). All of the sequences reported in this study clustered within the *Selenidium* clade from Pacific tube-forming polychaetes with very strong statistical support (Fig. 26). The *Selenidium* species isolated from serpulid polychaetes (*S. serpulae*, *S. sensimae* n. sp., *Selenidium* sp. 1 and *Selenidium* sp. 2) formed a robust subclade within the more inclusive *Selenidium* clade from Pacific tube-forming polychaetes. The two *Selenidium* species isolated from sipunculids (*S. orientale* and *S. pisinnus*) formed a separate clade that branched from an unresolved apicomplexan backbone; *S. terebellae*, isolated from a spaghetti worm (*Thelepus* sp.), did not cluster with either of the two *Selenidium* clades (Fig. 26). Our analyses also recovered separate clades consisting of coccidians, cryptosporidians, rhytidocystids, and two different compositions of terrestrial gregarines (terrestrial gregarines I and II). Generally speaking, statistical support values for branches reflecting more recent relationships were strong, but the overall apicomplexan backbone was poorly resolved (Fig. 26).

Molecular phylogenetic analyses of the 17-taxon alignment focused on the internal relationships within the *Selenidium* clade from Pacific tube-forming polychaetes and contained all of the SSU rDNA sequences derived from SC-PCR and four SSU rDNA sequences from previous work. These analyses resulted in distinct and well-supported subclades of *Selenidium* species that correlated with host affiliation and trophozoite morphology (Fig. 27). Genetic distances between the SSU rDNA sequence of *Selenidium* sp. 2 and all other *Selenidium* species in the analysis ranged from 8.3% to 14.0%; intraspecific variation between the SC isolates of *Selenidium* sp. 2 ranged from 0.3% to 0.8% (Table 2). Genetic distances between the SSU rDNA sequence of *Selenidium* sp. 1 and all other *Selenidium* species in the analysis ranged from 4.8% to 11.5%; intraspecific variation between the SC isolates of *Selenidium* sp. 1 ranged from 0.18% to 0.48% (Table 2). Genetic distances between the SSU rDNA sequence of *S. sensimae* n. sp. and all other *Selenidium* species in the analysis ranged from 5.8% to 12.8%; intraspecific variation between the SC isolates of *S. sensimae* n. sp. was 0.6% (Table 2). Genetic distances between the SSU rDNA sequence of *Selenidium* cf. *echinatum* and all other *Selenidium* species in the analysis ranged from 8.9% to 11.0%; intraspecific variation between the SC isolates of *S.* cf. *echinatum* n. sp. was 1.7% (Table 2). The lowest interspecific genetic distance found within this clade ranged from 2.2% to 2.4%, between *S. neosabellariae* n. sp. and *S. indanthyrsae*. Intraspecific variation between the SC isolates of *S. neosabellariae* n. sp. ranged from 0.24% to 0.42% (Table 2).

DISCUSSION

The majority of species descriptions within *Selenidium*, and gregarines in general, are based on morphological observations using light microscopy, electron microscopy, and line drawings (Levine 1971, 1976, 1977a,b, 1981; Ray 1930 Schrével 1968, 1971a,b; Vivier and Schrével 1964). Linking these older species descriptions to modern day species-discovery surveys is challenging because definitive traits for species identification are often lacking, especially when new isolates have been collected in environments that are very distant from the type locality. For instance, how does one reconcile a new Pacific isolate that is very similar in morphology to a gregarine species described from an Atlantic type locality? This issue is made increasingly formidable because: (1) infection rates may be low both within an individual host, and among a host population; (2) gregarines have never been cultivated; (3) different life history stages of gregarines are either ambiguous or difficult to observe

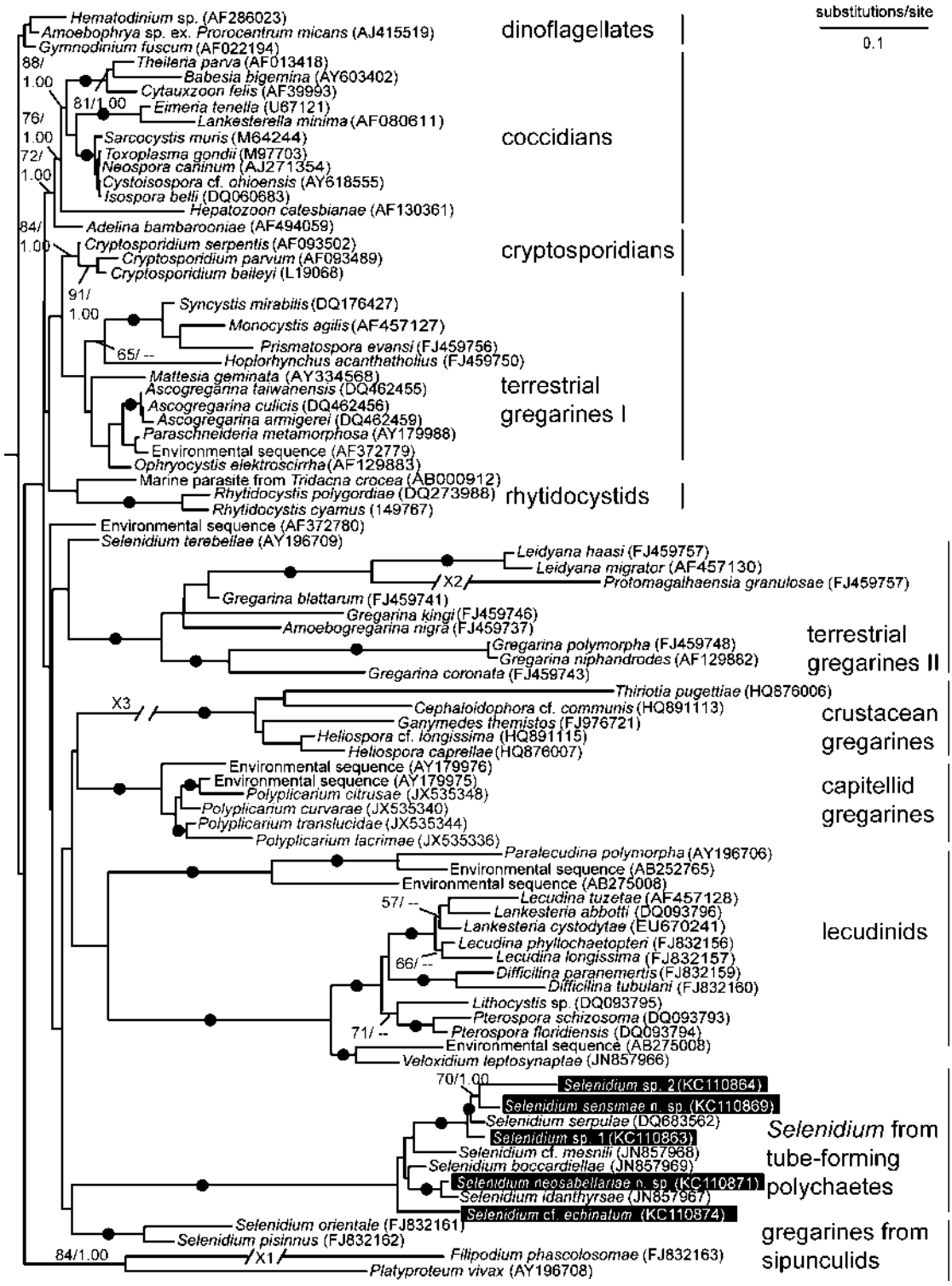

Figure 26 Maximum likelihood (ML) tree derived from phylogenetic analysis of the 82-taxon dataset (1,085 unambiguously aligned sites) of small subunit (SSU) rDNA sequences. This tree was inferred using the GTR + I + Γ substitution model (−ln *L*= 21,138.89056 gamma shape = 0.6230, proportion of invariable sites = 0.1820). Bootstrap support values are listed above Bayesian posterior probabilities are listed below. Black dots on branches denote bootstrap support values and Bayesian posterior probabilities of 95/0.95 or greater, respectively. Bootstrap and Bayesian values less than 55 and 0.95, respectively, were not added to this tree. Representative sequences from the five species of *Selenidium* described in this study are highlighted in black boxes. Some branches were shortened by the length (e.g., X1) of the substitutions/site scale bar.

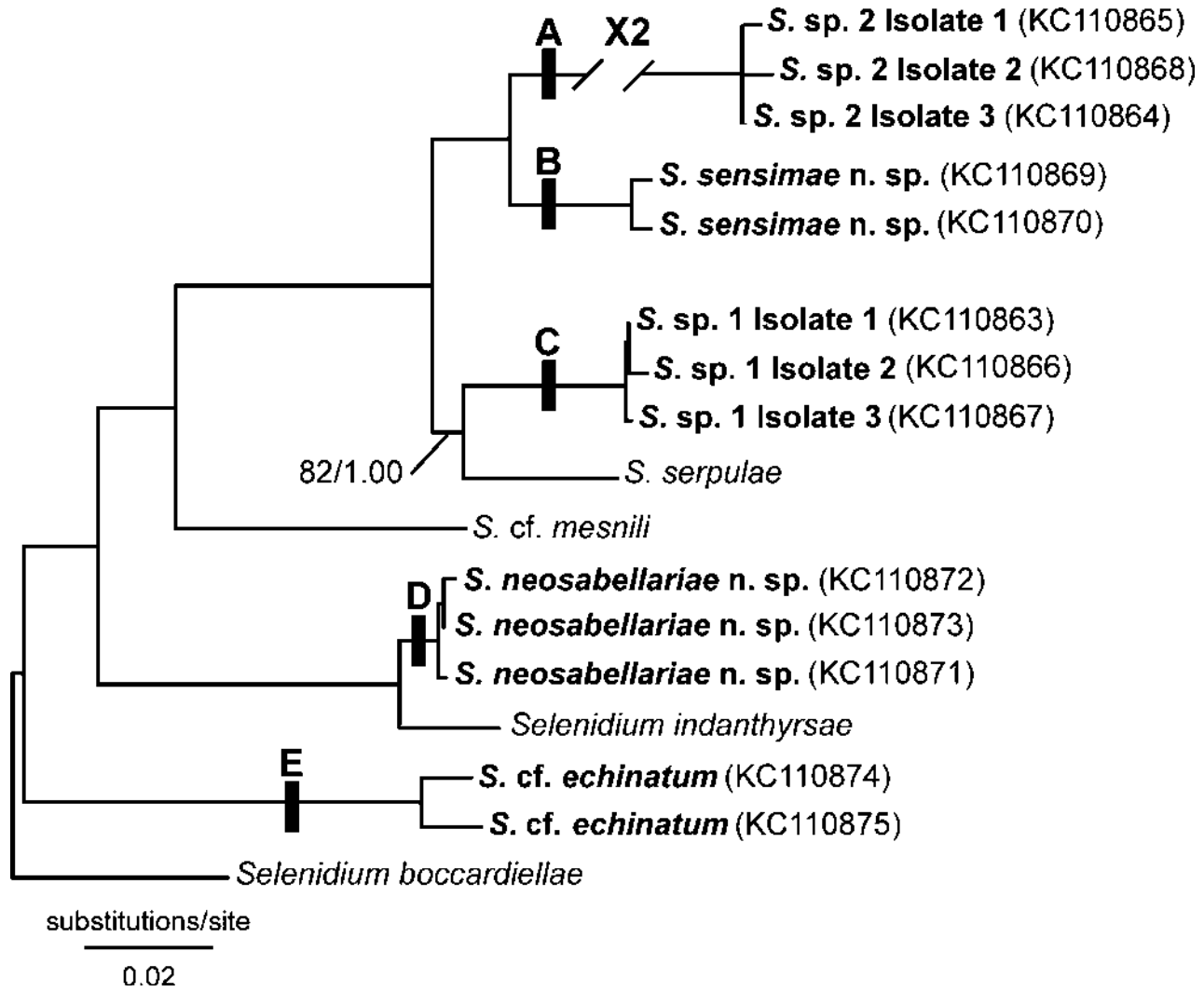

Figure 27 Unrooted maximum likelihood (ML) tree derived from phylogenetic analysis of the 17-taxon dataset (1,610 unambiguously aligned sites) containing small subunit (SSU) rDNA sequences from 13 single-cell isolates representing the five species of *Selenidium* described here (bold) and four closely related species of *Selenidium* published previously. This tree was inferred using the GTR + I + Γ substitution model (−ln L = 5,903.65704, gamma shape = 0.3770, proportion of invariable sites = 0.3290). Bootstrap support values are listed above Bayesian posterior probabilities; support values of 100 and 1.00 for bootstap and Bayesian analyses, respectively, are represented by black dashes. Morphological traits that distinguish the species from one another are indicated by letters. (**A**) Spindle-shaped trophozoites, 160 μm long and 13 μm wide, with spade-like posterior end; host: *Spirobranchus giganteus*. (**B**) Spindle-shaped trophozoites, 155 μm long and 12 μm wide, with blunt posterior end containing a terminal indentation; host: *S. giganteus*. (**C**) Vermiform trophozoites, 170 μm long and 13 μm wide, with bulbous posterior and anterior ends; host: *S. giganteus*. (**D**) Vermiform trophozoites, 292 μm long and 10 μm wide, with a pointed posterior end and a cluster of transverse striations that define the base of a nipple-like mucron; host: *Neosabellaria cementarium*. (**E**) Spindle-shaped trophozoites, 173 μm long and 10 μm wide, with pointed posterior end, a nipple-like mucron, and five to six subtle epicytic folds on each side of the cell; host: *Dodecaceria concharum*. Some branches were shortened by multiple lengths (e.g., X2) of the substitutions/site scalebar.

within an individual host; and (4) host material may be rare and only opportunistically available (e.g., acquired from a marine sediment dredge).

The literature is rich with examples of how molecular phylogenetic data can discriminate different species of microbial eukaryotes (protists) from one another, especially species that are rarely encountered, have very dissimilar life history stages, and are prone to cryptic speciation and convergent evolution (Adl et al. 2007; LaJeunesse et al. 2012). Along these lines, the use of molecular markers, especially SSU rDNA sequences, for evaluating the diversity of marine gregarines has been very informative for delimiting closely related species from one another and for discovering major clades of gregarine species (Leander et al. 2003; Rueckert and Leander 2010; Rueckert et al. 2010, 2011a,b, 2012; Wakeman and Leander 2013). Genetic distances have also shed light onto patterns of biogeography and host affinity in different

Table 2. Summary of percent sequence divergences of small subunit rDNA sequences from different species of *Selenidium*

	***Selenidium*. sp. 2**	***Selenidium*. sp. 1**	***Selenidium sensimae* n. sp.**	*Selenidium serpulae*	***Selenidium* cf. *echinatum***	*Selenidium* cf. *mesnili*	*Selenidium boccardiellae*	***Selenidium neosabellariae* n. sp.**	*Selenidium idanthyrsae*
***Selenidium* sp. 2**	0.30–0.80%								
***Selenidium* sp. 1**	9.1–9.8%	0.18–0.48%							
***Selenidium sensimae* n. sp.**	8.3–9.0%	5.7–6.1%	0.60%						
Selenidium serpulae	8.5–9.1%	4.8–5.1%	5.8%	N/A					
Selenidium* cf. *echinatum	13.4–14.0%	11.2–11.5%	12.7–12.8%	11.9–12.1%	1.7%				
Selenidium cf. *mesnili*	11.7–12.2%	9.2–9.5%	10.1%	9.1%	10.9–11.0%	N/A			
Selenidium boccardiellae	12.2–12.6%	9.9–10.2%	10.3%	9.6%	8.9–9.0%	8.2%	N/A		
***Selenidium neosabellariae* n. sp.**	12.3–12.8%	10.1–10.4%	10.4–10.5%	9.7–9.8%	10.2–10.7%	8.7–8.8%	8.2–8.3%	0.24–0.42%	
Selenidium idanthyrsae	12.4–12.7%	10.5–10.8%	10.9%	10.0%	10.3–10.6%	9.0%	9.0%	2.2–2.4%	N/A

The five *Selenidium* dicussed in this study are shown in bold font. Percent divergences are based on an alignment across 1,685 nucleotides. Intraspecific variation among sequences from four single-cell isolates of each new species are indicated along the diagonal.

gregarine species (Landers and Leander 2005; Leander et al. 2003; Rueckert et al. 2011b).

The variation in the SSU rDNA sequences generated here combined with host affinity, type locality, and trophozoite morphology suggest that all five gregarine morphotypes discovered in this study are different species. Two of the host species, namely *N. cementarium* and *S. giganteus*, were examined for gregarines for the first time in this study. A previous study of *D. concharum* in 1899 resulted in the description of one *Selenidium* species, namely *S. echinatum* (Caullery and Mesnil 1899). While the type locality of this species is in the Eastern Atlantic Ocean, the trophozoites we encountered within the intestines of *D. concharum* collected from the Eastern Pacific Ocean shared general morphological features with the original line drawings and description of *S. echinatum*: 10–12 longitudinal epicytic folds, spindle-shape, and tail-to-tail syzygy (Caullery and Mesnil 1899). Therefore, we chose to designate our isolate "*S.* cf. *echinatum*" until molecular phylogenetic data from gregarines isolated from *D. concharum* collected in the type locality have been generated; these data will further our understanding of biogeographical patterns associated with *Selenidium* species.

The trophozoites of *S. neosabellariae* n. sp. were isolated from the intestines of the tube worm *N. cementarium*, which is closely related to the type host of *Selenidium indanthyrsae*, namely *Idanthyrsus saxicavus* (Wakeman and Leander 2012). The SSU rDNA sequences from these two *Selenidium* species were also very similar, with a genetic distance of only 2.2–2.4%. However, intraspecific variability within the three different sequences of *S. neosabellariae* ranged from 0.24% to 0.42%, and the sequences formed a robust clade to the exclusion of *S. indanthyrsae* in the molecular phylogenetic analyses (Fig. 27). Moreover, along with an affiliation with different host species, the trophozoites of these two gregarine species can be distinguished from one another at the morphological level; the trophozoites of *S. neosabellariae* n. sp. are half the average length and have half the number of longitudinal folds (visible) as the trophozoites of *S. indanthyrsae* (Table 1).

The three different morphotypes of trophozoites discovered within the intestines of *S. giganteus* also had distinctive SSU rDNA sequences, which taken together formed the basis for establishing *S. sensimae* n. sp. and the recognition of two additional putative species (*Selenidium* sp. 1 and 2). Differences in the form of the posterior end of the trophozoites between *S. sensimae* n. sp., *Selenidium* sp. 1, and *Selenidium* sp. 2 were diagnostic for each: *Selenidium* sp. 1 has a bulbous posterior end, *Selenidium* sp. 2 has a spade-like posterior end, and *S. sensimae* n. sp. has a posterior end that tapers to a blunt point with a terminal indentation. A more focussed molecular phylogenetic analyses of the SSU rDNA sequences from these three species (in the 17-taxon alignment) allowed us to include almost 600 additional homologous sites (compared to the more comprehensive 82-taxon alignment consisting of more distantly related gregarines and apicomplexans). The

17-taxon alignment resulted in robust clades that were congruent with the observed morphological difference between the trophozoites. Interspecific variability between these three clades ranged from 5.7% to 9.8%, while intraspecific variability ranged from 0.18% to 0.80% (Table 2 and Fig. 27). The intraspecific variation between the SC isolates was localized to the hyper-variable regions in the SSU rDNA sequences (i.e., not randomly scattered throughout the sequences). Similarly, most of the sequences from the SC isolates of each morphotype shared identical indels and nucleotide substitutions. These results indicate that this variability reflects the population rather than artifacts of PCR or sequencing error. Nonetheless, the hyper-variable regions and ambiguous sites (e.g., indels) were excluded from the phylogenetic analyses.

Molecular phylogenetic analyses of the 82-taxon alignment, including representative sequences from each of the five morphotypes discovered in the study, demonstrated a robust clade of nine *Selenidium* species isolated from Pacific tube-forming polychaetes. This clade does not include *Selenidium* species collected from sipunculids (*S. orientale* and *S. pisinnus*) or other lineages of polychaetes such as spaghetti worms (*S. terebellae*). As such, these data demonstrate that host affinity can be a predictor of gregarine phylogenetic relationships and offers additional insights into emerging co-evolutionary patterns between gregarine parasites and their marine invertebrate hosts. The (unresolved) phylogenetic positions of *S. terebellae, Veloxidium leptosynaptae*, and the clade consisting of *S. orientale* and *S. pisinnus* leave open the possibility that the *Selenidium* morphotype (i.e., the "archigregarine" concept) reflects a paraphyletic stem group from which all other gregarines, and perhaps apicomplexans, generally evolved (Leander 2008; Wakeman and Leander 2012). Phylogenetic analyses of additional molecular markers (e.g., heat shock protein 90 and perhaps cytoskeletal protein genes) from *Selenidium* species offer the most promising way forward for evaluating the strength of the phylogenetic hypotheses inferred from SSU rDNA sequences.

It is worthwhile to note here that an article published this year (Clopton 2012) argued strongly against the predominant use of molecular phylogenetic data for describing gregarine species, and perhaps organisms in general, in favor of a set of ideological rules based on detailed analyses of morphometric data; the promotion of these rules is intended to govern the way new species of gregarines should be described in the future. As reflected in our previous studies (Landers and Leander 2005; Leander 2007; Leander et al. 2003; Rueckert and Leander 2010; Rueckert et al. 2010, 2011a,b, 2012; Wakeman and Leander 2012, 2013), we advocate a very different point of view and path forward using SC-PCR and comparative analyses of molecular markers (e.g., SSU rDNA) to more precisely determine the boundaries between gregarine species. The advantages and insights gained from molecular data are varied and have been repeatedly demonstrated in a large body of molecular systematic studies on a vast array of lineages (e.g., determining biogeographical patterns, convergent evolution of morphological traits, cryptic species, and the connections between disparate life history stages of the same species) (Bucklin et al. 2011; Hebert and Gregory 2005; Pawlowski et al. 2012).

Molecular phylogenetic approaches are particularly powerful and pragmatic for the systematics of gregarine parasites because their life histories involve several distinct developmental stages (e.g., cysts, sprorozoites, and trophozoites at different phases of maturation) that complicate species identification based on morphology alone, no matter how detailed the morphometric data might be (Leander 2008; Rueckert et al. 2011b; Wakeman and Leander 2013). Moreover, not all life history stages are available to observe at any given time (especially in species of marine gregarines) and there tends to be high levels of intraspecific variation coupled with low levels of interspecific variation associated with trophozoite morphology, which is the most conspicuous life history stage in most gregarine species. The SSU rDNA sequences reported here from *S.* cf. *echinatum* provide an important example of how molecular data will help us reconcile new discoveries with previous species descriptions based on line drawings and/or light micrographs. The SSU rDNA sequences from our Pacific Ocean isolates can eventually be compared with SSU rDNA sequences generated from isolates of *S. echinatum* collected from hosts living in the type locality in the Atlantic Ocean. We were unable to make a definitive species identification based on comparative morphology alone because of the ambiguities associated with the trophozoite traits and the original description itself. The intraspecific and interspecific variation associated with molecular markers, such as SSU rDNA sequences, will provide great insight into whether or not *S. echinatum* has a biogeographical distribution that extends into both the Pacific and Atlantic Oceans or represents two different (cryptic) species. The SSU rDNA sequence data also place the diversity of gregarine species into a molecular phylogenetic context, which so far has demonstrated several unexpected clades and relationships that are steadily refining our overall understanding of apicomplexan evolution.

TAXONOMIC SUMMARY

Apicomplexa Levine, 1970
  Gregarinea Bütschli, 1882, stat. nov. Grassé 1953
  Archigregarinorida Grassé 1953
  Selenidiidae Brasil, 1907
  Selenidium Giard, 1884

Selenidium neosabellariae n. sp. Wakeman and Leander

Description. Trophozoites vermiform with an average length and width, at the widest part, of 292 μm and 11 μm, respectively. Cells light-brown. The posterior end tapers to a fine point; the anterior end tapers to a cone-shaped mucron defined at the base by a series of

transverse striations. A spherical nucleus (10 × 12–14 μm) is positioned in the center of the cell. Trophozoites move by undulating, bending and twisting. Five to six deep longitudinal striations occur on each side of the trophozoite surface.

DNA sequence. SSU rDNA sequence (GenBank KC110871).

Type locality. Ogden Point (48°24′46.10″N 123°23′24.67″W), Victoria, British Columbia, Canada. Host in tubes on rocks; subtidal; 20 m below mean sea level.

Type habitat. Marine.

Type host. *Neosabellaria cementarium* Moore, 1906 (Annelida, Polychaeta, Sabellida, Sabellariidae).

Location in host. Intestinal lumen.

Type material. Parasites on gold sputter-coated SEM stubs have been deposited in the Beaty Biodiversity Museum (Marine Invertebrate Collection) at the University of British Columbia, Vancouver, Canada. Museum Code – MI-PR122. This accession constitutes the name-bearing hapantotype for this species, and is represented by Fig. 12.

Etymology. The species name, *neosabellariae*, refers to the genus of the type host.

Selenidium sensimae n. sp. Wakeman and Leander

Description. Trophozoites spindle-shaped with an average length and width, at the widest part, of 155 μm and 12 μm, respectively. Cells dark-brown. An ellipsoidal nucleus (10 × 4–6 μm) is positioned in the central part of the cell. The posterior end of the cell tapers to a blunt point with a terminal indentation; the anterior region of the cell forms a rounded or pointed mucron. Trophozoites bend and twist slowly. Eight to nine longitudinal striations occur on each side of the trophozoite surface.

DNA sequence. SSU rDNA sequence (GenBank KC110863).

Type locality. Coral specimen purchased from J&L Aquatics, Burnaby, British Columbia, Canada, collected in the Eastern Pacific Ocean (Fiji) in coral reef habitat.

Type habitat. Marine.

Type host. *Spirobranchus giganteus* Pallas, 1766 (Annelida, Polychaeta, Sabellida, Serpulidae).

Location in host. Intestinal lumen.

Type Material. Parasites on gold sputter-coated SEM stubs have been deposited in the Beaty Biodiversity Museum (Marine Invertebrate Collection) at the University of British Columbia, Vancouver, Canada. Museum Code – MI-PR123. This accession constitutes the name-bearing hapantotype for this species, and is represented by Fig. 18.

Etymology. The specific epithet, *sensimae*, means "slowly" in Latin and refers to the slow bending and twisting movements observed in the trophozoites.

ACKNOWLEDGMENTS

This research was supported by grants from the National Science and Engineering Research Council of Canada (NSERC 283091-09) and the Canadian Institute for Advanced Research, Program in Integrated Microbial Biodiversity.

LITERATURE CITED

Adl, S. M., Leander, B. S., Simpson, A. G. B., Archibald, J. M., Anderson, O. R., Bass, D., Bowser, S. S., Brugerolle, G., Farmer, M. A., Karpov, S., Kolisko, M., Lane, C. E., Lodge, D. J., Mann, D. G., Meisterfeld, R., Mendoza, L., Moestrup, Ø., Mozley-Standridge, S. E., Smirnov, A. V. & Spiegel, F. 2007. Diversity, nomenclature, and taxonomy of protists. *Syst. Biol.*, 56:684–689.

Barta, J. R. & Thompson, R. C. A. 2006. What is *Cryptosporidium*? Reappraising its biology and phylogenetic affinities. *Trends Parasitol.*, 22:463–468.

Brasil, L. 1909. Documents sur quelques sporozoaires d'annélides. *Arch. Protistenk.*, 16:107–142.

Bucklin, A., Steinke, D. & Blanco-Bercial, L. 2011. DNA barcoding of marine metazoa. *Annu. Rev. Marine. Sci.*, 3:471–508.

Caullery, M. & Mesnil, F. 1899. Sur quelques parasites internes des annélids. I. Les grégarines nématoïdes des annélids: *G.* Selenidium Giard. *Trav. Stat. Zool. Wimereux*, 7:80–99.

Clopton, R. E. 2012. Synoptic revision of *Blabericola* (Apicomplexa: Eugregarinida: Blabericolidae) parasitizing blaberid cockroaches (Dictyoptera: Blaberidae), with comments on delineating gregarine species boundaries. *J. Parasitol.*, 98:572–583.

Cox, F. E. G. 1994. The evolutionary expansion of the Sporozoa. *Int. J. Parasitol.*, 24:1301–1316.

Dyson, J., Grahame, J. & Evennett, P. J. 1994. The apical complex of the gregarine *Digyalum oweni* (Protozoa, Apicomplexa). *J. Nat. Hist.*, 28:1–7.

Edgar, R. C. 2004. MUSCLE: multiple sequence alignment with high accuracy and high throughput. *Nucleic Acids Res.*, 32:1792–1797.

Grassé, P.-P. 1953. Classe des grégarinomorphes (Gregarinomorpha, N. nov., Gregarinae Haeckel, 1866; gregarinidea Lankester, 1885; grégarines des auteurs). *In*: Grassé, P.-P. (ed.), Traité de Zoologie. Masson, Paris. p. 590–690.

Hebert, P. D. N. & Gregory, T. R. 2005. The promise of DNA barcoding for taxonomy. *Syst. Biol.*, 54:852–859.

Huelsenbeck, J. P. & Ronquist, F. 2001. MrBayes: Bayesian inference of phylogenetic trees. *Bioinformatics*, 17:754–755.

Landers, S. C. & Leander, B. S. 2005. Comparative surface morphology of marine coelomic gregarines (Apicomplexa, Urosporidae): *Pterospora floridiensis* and *Pterospora schizosoma*. *J. Eukaryot. Microbiol.*, 52:23–30.

LaJeunesse, T. C., Parkinson, J. E. & Reimer, J. D. 2012. A genetics-based description of *Symbiodinium minutum* sp. nov. and *S. psygmophilum* sp. nov. (Dinophyceae), two dinoflagellates symbiotic with cnidaria. *J. Phycol.*, 1–12.

Leander, B. S. 2006. Ultrastructure of the archigregarine *Selenidium vivax* (Apicomplexa) – a dynamic parasite of sipunculid worms (Host: *Phascolosoma agassizii*). *Mar. Bio. Res.*, 2:178–190.

Leander, B. S. 2007. Molecular phylogeny and ultrastructure of *Selenidium serpulae* (Apicomplexa, Archigregarinia) from the calcareous tubeworm *Serpula vermicularis* (Annelida, Polychaeta, Sabellida). *Zool. Scripta*, 36:213–227.

Leander, B. S. 2008. Marine gregarines – evolutionary prelude to the apicomplexan radiation? *Trends Parasitol.*, 24:60–67.

Leander, B. S., Harper, J. T. & Keeling, P. J. 2003. Molecular phylogeny and surface morphology of marine aseptate gregarines

(Apicomplexa): *Selenidium* spp. and *Lecudina* spp. *J. Parasitol.*, 89:1191–1205.
Leander, B. S. & Keeling, P. J. 2003. Morphostasis in alveolate evolution. *Trends Ecol. Evol.*, 18:395–402.
Levine, N. D. 1971. Taxonomy of Archigregarinorida and Selenidiidae (Protozoa, Apicomplexa). *J. Protozool.*, 18:704–717.
Levine, N. D. 1976. Revision and checklist of the species of the aseptate gregarine genus *Lecudina*. *Trans. Am. Microsc. Soc.*, 95:695–702.
Levine, N. D. 1977a. Revision and checklist of the species (other than *Lecudina*) of the aseptate gregarine family Lecudinidae. *J. Protozool.*, 24:41–52.
Levine, N. D. 1977b. Checklist of the species of the aseptate gregarine family Urosporidae. *Int. J. Parasitol.*, 7:101–108.
Levine, N. D. 1981. New species of *Lankesteria* (Apicomplexa, Eugregarinida) from ascidians on the central California coast. *J. Protozool.*, 28:363–370.
Maddison, D. R. & Maddison, W. P. 2000. MacClade 4. Sinauer Associates, Sunderland.
Mellor, J. S. & Stebbings, H. 1980. Microtubules and the propagation of bending waves by the archigregarine, *Selenidium fallax*. *J. Exp. Biol.*, 87:149–161.
Pawlowski, J., Audic, S., Adl, S., Bass, D., Belbahri, L., Berney, C., Bowser, S. S., Cepicka, I., Decelle, J., Dunthorn, M., Fiore-Donno, A. M., Gile, G. H., Holzmann, M., Jahn, R., Jirků, M., Keeling, P. J., Kostka, M., Kudryavtsev, A., Lara, E., Lukeš, J., Mann, D. G., Mitchell, E. A., Nitsche, F., Romeralo, M., Saunders, G. W., Simpson, A. G., Smirnov, A. V., Spouge, J. L., Stern, R. F., Stoeck, T., Zimmermann, J., Schindel, D. & de Vargas, C. (2012) CBOL Protist Working Group: barcoding eukaryotic richness beyond the animal, plant, and fungal kingdoms. *PLoS Biol.*, 10:e1001419.
Posada, D. & Crandall, K. A. 1998. MODELTEST: testing the model of DNA substitution. *Bioinformatics*, 14:817–818.
Ray, H. N. 1930. Studies on some protozoa in polychaete worms. I. Gregarines of the genus *Selenidium*. *Parasitology*, 22:370–400.
Ronquist, F. & Huelsenbeck, J. P. 2003. MRBAYES 3: Bayesian phylogenetic inference under mixed models. *Bioinformatics*, 19:1572–1574.
Rueckert, S., Chantangsi, C. & Leander, B. S. 2010. Molecular systematics of marine gregarines (Apicomplexa) from Northeastern Pacific polychaetes and nemerteans, with descriptions of three new species: *Lecudina phyllochaetopteri* sp. nov., *Difficilina tubulani* sp. nov., and *Difficilina paranemertis* sp. nov. *Int. J. Syst. Evol. Microbiol.*, 60:2681–2690.
Rueckert, S. & Leander, B. S. 2009. Molecular phylogeny and surface morphology of marine archigregarines (Apicomplexa), *Selenidium* spp., *Filipodium phascolosomae* n. sp., and *Platyproteum* n. gen. and comb. from north-eastern pacific peanut worms (Sipuncula). *J. Eukaryot. Microbiol.*, 56:428–439.
Rueckert, S. & Leander, B. S. 2010. Description of *Trichotokara nothriae* n. gen. et sp. (Apicomplexa, Lecudinidae) – an intestinal gregarine of *Nothria conchylega* (Polychaeta, Onuphidae). *J. Invert. Path.*, 104:172–179.
Rueckert, S., Villette, P. & Leander, B. S. 2011a. Species boundaries in gregarine apicomplexans: a case study comparison of morphometric and molecular variability in *Lecudina* cf. *tuzetae* (Eugregarina, Lecudinidae). *J. Eukaryot. Microbiol.*, 58:275–283.
Rueckert, S., Simdyanov, T. G., Aleoshin, V. V. & Leander, B. S. 2011b. Identification of a divergent environmental DNA sequence clade using the phylogeny of gregarine parasites (Apicomplexa) from crustacean hosts. *PLoS ONE*, 6:e18163.
Rueckert, S., Wakeman, K. C. & Leander, B. S., 2012. Discovery of a diverse clade of gregarine apicomplexans from Pacific eunicid and onuphid polychaetes, including descriptions of *Paralecudina* gen. n., *Trichotokara japonica* n. sp., and *T. eunicae* n. sp. . *J. Eukaryot. Microbiol.*, 60:121–136.
Schrével, J. 1968. L'ultrastructure de la région antérieure de la grégarine *Selenidium* et son intérêt pour l'étude de la nutrition chez les sporozoaires. *J. Microsc. Paris*, 7:391–410.
Schrével, J. 1970. Contribution a l'étude des Selenidiidae parasites d'annélides polychè tes. I. Cycles biologiques. *Protistologica*, 6:389–426.
Schrével, J. 1971a. Observations biologique et ultrastructurales sur les Selenidiidae et leurs conséquences sur la systématique des grégarinomorphes. *J. Protozool.*, 18:448–470.
Schrével, J. 1971b. Contribution a l'étude des Selenidiidae parasites d'annélides polychètes. II. Ultrastructure de quelques trophozoïtes. *Protistology*, 7:101–130.
Simdyanov, T. G. & Kuvardina, O. N. 2007. Fine structure and putative feeding mechanism of the archigregarine *Selenidium orientale* (Apicomplexa: Gregarinomorpha). *Eur. J. Protistol.*, 43:17–25.
Stebbings, H., Boe, G. S. & Garlick, P. R. 1974. Microtubules and movement in the archigregarine, *Selenidium fallax*. *Cell Tissue Res.*, 148:331–345.
Swofford, D. L., 1999. Phylogenetic Analysis Using Parsimony (and Other Methods) PAUP* 4.0. Sinauer Associates, Inc.: Sunderland, MA.
Théodoridès, J. 1984. The phylogeny of the Gregarinia. *Orig. Life*, 13:339–342.
Vivier, E. & Schrével, J. 1964. Étude au microscope électronique de une grégarine du genre *Selenidium*, parasite de *Sabellaria alveolata*. *J. Microsc. Paris*, 3:651–670.
Wakeman, K. C. & Leander, B. S. 2012. Molecular phylogeny of pacific archigregarines (Apicomplexa), including descriptions of *Veloxidium leptosynaptae* n. gen., n. sp., from the sea cucumber *Leptosynapta clarki* (Echinodermata), and two new species of *Selenidium*. *J. Eukaryot. Microbiol.*, 59:232–45.
Wakeman, K. C. & Leander, B. S. 2013. Identity of environmental DNA sequences using descriptions of four novel gregarine parasites, *Polyplicarium* n. gen. (Apicomplexa), from capitellid polychaetes. *Mar. Biodiv.*, 43:133–147.
Zwickl, D., 2006. Genetic algorithm approaches for the phylogenetic analysis of large biological sequence datasets under the maximum likelihood criterion. Ph.D. Thesis. University of Texas, Austin.